JOURNAL OF MATERIALS SCIENCE 19 (1984) 3574–3587

The Ni_3Al–Ni_3Cr–Ni_3Mo section of the Ni–Cr–Al–Mo system

S. CHAKRAVORTY, D. R. F. WEST
Department of Metallurgy and Materials Science, Imperial College of Science and Technology, London SW7 2BX, UK

An investigation is reported of the constitution of the 75 at% nickel section of the Ni–Cr–Al–Mo system in the temperature range 1523 to 1073 K. Alloys in the region 10 to 20 at% Al were annealed at 1523, 1273, and 1073 K, respectively, and subjected to electron microprobe analysis, X-ray diffraction, and microscopical and hardness examination. Constitutional data are presented as partial isothermal sections and as vertical sections. At 1523 K the section consists only of fields containing γ', $\gamma' + \gamma$ and γ, the last mentioned phase being predominant. With decreasing temperature the γ' and $\gamma' + \gamma$ fields increase in extent. Also, the NiMo and Ni_3Mo phases were encountered in the ternary Ni–Al–Mo alloy studied. The quaternary $\gamma + \gamma'$ alloys showed small lattice mismatch values, i.e. up to ~ 0.25%. Raft like morphologies of γ' were found in the quaternary alloys, resulting from directional coarsening. Observations of as-cast structures are also reported.

1. Introduction

In understanding the equilibrium constitution of multi-component nickel based superalloys various quaternary systems can provide important insights. The Ni–Cr–Al–Mo system is of particular interest in representing the equilibria between γ (nickel-rich solid solution), γ' (based on Ni_3Al) and σ phases. Machlin and Shao [1] have proposed the extension of the Ni–Cr–Al–Mo quaternary to higher order alloys by using the following scheme of equivalents: (Ni, Co, Fe):Cr:(Al, Ti):(Mo, W, Nb, V, Ta, Hf). They have discussed a procedure termed SIGMA-SAFE to predict the tendency to σ precipitation in individual alloys. The boundaries between the γ, $\gamma + \sigma$, $\gamma + \gamma'$ and $\gamma + \gamma' + \sigma$ phase fields in the multi-component phase diagrams corresponding to superalloy compositions have been predicted as a function of temperature. Machlin and Shao [1] have given a schematic representation of the nickel-rich corner of the quaternary Ni–Cr–Al–Mo system. However, there appear to be no experimental determinations reported of the equilibrium diagram of the system and the present investigation aimed to obtain such data for the nickel-rich portion.

The experimental approach adopted in the presently reported work is to determine parts of isothermal sections in the range 1523 to 1073 K at selected constant nickel contents; two series of alloys were selected for this purpose. The first series, which is reported here, lies on the 75 at% Ni section of the quaternary, and serves to represent the γ/γ' equilibria. The second series, with 50 or 60 at% Ni, includes σ and P phase equilibra; the results are to be reported separately. The use of electron microprobe analysis to establish tie lines enables isothermal section data to be obtained from a relatively small number of alloys.

2. Literature survey

The literature concerning the nickel-rich corners of the Ni–Al–Cr, Ni–Al–Mo and Ni–Cr–Mo ternary systems is selectively reviewed here to provide a basis for considering the equilibria relevant to the 75 at% Ni section of the quaternary system.

2.1. Ni–Al–Cr system

The literature on the complete system (e.g. [2–11]) has recently been the subject of a detailed

0022–2461/84 $03.00 + .12 © *1984 Chapman and Hall Ltd.*

critical assessment by Merchant and Notis [12]; isothermal section data exist mainly for the region NiAl–Cr–Ni. An extensive investigation by Taylor and Floyd [2] covered the temperature range 1423 to 1023 K and included tie-line data, e.g. for γ/γ' equilibria, based on X-ray measurements. They also presented a possible form of the liquidus projection. Part of an isothermal section at 1473 K was determined by Kornilov and Mints [4, 7] and the maximum solubility of chromium in γ' was found to be ~ 7.8 at%. The assessment of Merchant and Notis refers to recent work by DeLanerolle and Seigle [13] and by Tu [14] on the 1298 K section. Another recent investigation of the system is that of Argent *et al.* [15] who have studied the isothermal section at 1423 K. Among features of interest from previous investigations is an invariant reaction at ~ 1273 K: $\beta(\text{NiAl}) + \gamma \rightarrow \gamma' + \text{Cr}$ (solid solution) [2]; below this temperature the system includes three phase equilibria between β, γ and γ' and β, γ and Cr.

As far as the 75 at% Ni line is concerned the range of the present work includes single phase regions of γ and γ', respectively, and a two-phase $\gamma + \gamma'$ region. At 1523 K the γ range is very wide but its extent is greatly reduced with decreasing temperature. The solubility of chromium in γ' increases with decreasing temperature approaching 20 at% at 1023 K [2].

2.2. Ni–Al–Mo system

The literature on the nickel-rich corner has been recently summarized [16] and also some additional references should be noted [9, 17–25]. Nash *et al.* [24] determined a partial isothermal section at 1473 K which confirmed previous work except that the maximum solubility of molybdenum in γ' was found to be greater, at around 6 at%. The 75 at% Ni line at 1473 K is similar in general form to that in the Ni–Al–Cr system containing γ and γ' regions separated by a $\gamma + \gamma'$ region. As the aluminium and molybdenum contents are progressively increased three phase equilibria are encountered involving $\gamma + \gamma' + \text{Mo}$ and $\gamma' + \beta + \text{Mo}$: equilibrium between γ, Mo and NiMo is also inferred at 1473 K. A possible schematic form of the liquidus in the nickel-rich region was presented [24]. More recently Wakashima *et al.* [25] have reinvestigated the equilibria and have confirmed the occurrence of an invariant reaction: $\gamma + \text{Mo} \rightarrow \gamma' + \text{NiMo}$ at ~ 1400 K. Thus, the 75 at% Ni section below 1400 K includes a three phase region containing γ, γ' and NiMo. Miracle *et al.* [17] have also reported this invariant reaction at a temperature between ~ 1365 and 1420 K. Markiv *et al.* [18] have reported an isothermal section at 1073 K which shows the Ni_3Mo phase entering into equilibrium with γ and molybdenum and with NiMo and molybdenum.

2.3. Ni–Cr–Mo system

A detailed investigation of the constitution of the system at 1523 K has been reported by Bloom and Grant [26] following a previous study of part of the system at 1473 K [27, 28]. At 1523 K the γ phase was shown to enter into equilibria with the following phases: NiMo (δ'), P phase (a ternary compound), σ phase (another ternary compound) and the bcc solid solution involving chromium and molybdenum (which two elements show complete solid solubility). Sigma shows a very extensive single phase region, particularly with respect to chromium content (from ~ 22 to 60 at% Cr along a region located around a nickel content of ~ 32 at%). P phase lies between σ and δ' at around 40Ni–42Mo–18Cr (at%) at 1473 K [30]. The structures of both σ and P phases have been investigated in detail e.g. [29–31]. σ phase is reported as β-uranium type tetragonal structure $P4/mnm$ with $a = 0.900$ nm, $c = 0.450$ nm at a composition of ~ 27 Ni–27 Mo–46 Cr (at%) [27, 28]. P phase is reported as primitive orthohombic with $a = 0.9070$ nm, $b = 1.6983$ nm and $c = 0.4752$ nm, space group $D16/2h$-Pbnm [30].

Three phase regions at 1523 K include $\gamma + \text{NiMo} + \text{P}$; $\gamma + \text{P} + \sigma$ and $\gamma + \sigma + (\text{Cr, Mo})$. The 75 at% Ni line of the 1523 K isothermal, which is the only feature relevant to the present work, is shown as including a small amount of the $\gamma + \text{NiMo}$ region [26]. However, recent data [31] and the present work indicate that the solubility limit of molybdenum in nickel is greater than 25 at% so that the whole of the 75 at% Ni line is single phase γ. Various other studies of the constitution of the Ni–Cr–Mo system have been reported, including isothermal sections for various temperatures in the range 2400 to 1000 K, calculated from thermodynamic data [32]. Theoretical considerations of the γ boundary on the basis of PHACOMP techniques have been put forward by Barrows and Newkirk [33] and by Mihalisin *et al.* [34]; the latter have also presented an extrapolated γ phase boundary at 1173 K. Smiryagin *et al.* [35] determined the limits of the γ field in the range 973 to 1473 K.

The data obtained by Raghavan *et al.* [31] for the limit of the γ field at 1523 K agree quite well with the 1473 K results of Rideout *et al.* [28], except in the high chromium range. The limit is greater than that reported by Bloom and Grant for 1523 K [26].

As the temperature is progressively decreased below 1523 K phase fields involving NiMo, Ni_3Mo, and possibly P intrude into the 75 at% Ni line. Raghavan *et al.* [31] have reported that an additional phase forms at 1123 K, namely a μ phase (A_7B_6 type compound).

3. Experimental procedure

Three quaternary alloys were prepared along a line from the Ni_3Al corner of the 75 at% Ni section of the isothermal tetrahedron with decreasing aluminium contents and a constant ratio of chromium and molybdenum (Table I). Two ternary alloys were also prepared, one from the Ni–Al–Mo system and the other from the Ni–Al–Cr system; these alloys contained 15 at% Al in common with one of the quaternary alloys (Table I). The alloy-making employed metals of purity: nickel (99.99%), chromium (~ 99.9%); aluminium (99.99%) and molybdenum (~ 99.9%). Argon arc melting was used to produce ingots of ~ 30 g weight, several remelts being made to aid homogeneity. Melting losses in similar previous studies were usually < 1% by weight, but in the present series of alloy the losses were somewhat greater, i.e. up to ~ 1.5%.

Samples were cut from the ingots for examination. The remaining portion of the ingots were sealed in silica tube under vacuum with a partial pressure of argon; they were then annealed for 1 week at 1523 ± 5 K followed by iced water quenching. Portions were reheated to 1273 ± 5 K for 1 week and iced water quenched; after this treatment, portions were annealed for 1 week at 1073 ± 5 K and iced water quenched. Arising from studies on the Ni–Al–Mo–Ta system, the Ni–Al–Mo alloy (1) was also annealed at 1073 K for 1 week without prior treatment at 1273 K; this was done to approach equilibrium at 1073 K from a $\gamma + \gamma'$ structure without the presence of NiMo which forms during 1273 K anneal.

Optical and SEM examination were carried out on specimens etched with Marble's reagent or alcoholic ferric chloride ($FeCl_3$ 5 g, HCl 2 cm^3, ethanol 95 cm^3). Bulk polished samples were held on a rotary spinner for X-ray diffractometer examination using Cu$K\alpha$ radiation and a graphite monochromator. The lattice spacing values were estimated to have an accuracy better than ± ~ 0.2%. Electron microprobe analysis (EPMA) was carried out on polished, unetched samples by EDX analysis using a JEOL JSM-35CF instrument and a ZAF4 computer programme software disc supplied by LINK. The resolution for compositional analysis is ~ 2 μm and the relative error is < 1% of the individual element. Back scattered electron imaging was used to assist in characterizing the phases.

A minimum of 5 EDX analyses of each phase was made. Although coring was observed in some specimens after annealing, no concentration gradients were detected within individual phase regions after annealing, thus indicating local equilibrium. The agreement between analysed and nominal compositions was not as close as has been found in work on other similar systems, e.g. [16, 24]; the analysed aluminium contents were significantly lower than the nominal values and the analysed nickel contents higher than the nominal contents so that the second studied lies nearer to 76 at% Ni than 75 at% Ni. The differences tended to be more marked in the as-cast samples where the heterogeneity of structure was most noticeable and hence the analysis the least accurate.

4. Results and discussion

Tables I and II list X-ray, phase composition and hardness data. It should be noted that in some cases, the fine γ' particle size prevented accurate microprobe analysis not only of the γ', but sometimes of the matrix γ phase. Microstructural features are discussed in Section 4.4.

To assist in the interpretation of the data, Fig. 1 shows schematically information concerning the nickel-rich corner of the quaternary system. In the present work the following symbols are used for the Ni–Mo compounds. δ'-NiMo; δ''-Ni_3Mo; the symbol δ has been used for NiMo in some previous work in the literature [36, 37], but this is not followed here to avoid confusion with the compound Ni_3Ta which is often referred to as δ.

4.1. Isothermal sections (Figs. 2a to c)

At 1523 K the isothermal section is simple in form containing only the γ and γ' phases; the single phase γ region dominates the section. At 1273 and 1073 K the single phase γ' region has expanded

TABLE I Alloy compositions and hardness with phase structures and lattice parameters (nm)

Alloy number	Nominal Alloy Composition (at %)				Hardness (HV)				γ				γ' (based on Ni_3Al)				δ' (based on NiMo)	δ'' (based on Ni_3Mo)
									fcc				fcc				Pseudo-Orthogonal $a = b$ c	Orthogonal a b c
	Ni	Cr	Al	Mo	As-cast	1523 K	1273 K	1073 K	As-cast	1523 K	1273 K	1073 K	As-cast	1523 K	1273 K	1073 K	1273 K	1073 K
1	75	–	15	10	442	421	393	450‡	0.3598	0.3594	0.3610	0.3579‡	0.3579	0.3574	0.3580	0.3586‡	0.9178 0.8513	0.5067‡ 0.4182 0.4449
2	75	10	15	–	266	247	234	241	0.3568	0.3563	0.3557	0.3558	0.3559*	0.3557*	0.3561	0.3565		
3†	75	2.5	20	2.5	204	206	161	161	0.3575	0.3574			0.3566*	0.3568	0.3570	0.3572		
4	75	5	15	5	367	345	286	302	0.3580	0.3584	0.3581	0.3581	0.3573*	0.3575*	0.3574	0.3576		
5	75	7.5	10	7.5	333	289	233	335	0.3584	0.3587	0.3586	0.3586	0.3576*		0.3577	0.3580		

*Precipitated during quenching/cooling.

†Also β (based on NiAl) present in the as-cast condition; b c c CsCl type structure, $a = 0.2857$ nm.

‡The data refer to annealing at 1073 K without prior annealing at 1273 K.

TABLE II Alloy compositions and phase compositions

Alloy number	Alloy Treatment	Phases Present	Alloy Composition Determined by EPMA (at %) Ni– Cr – Al –Mo	Phase Composition Determined by EPMA (at %) Ni–Cr–Al–Mo			
				γ	γ'	δ'	δ''
1	As-cast	$\gamma + \gamma' + *$	76.1– 0 –13.4–10.5	72.1– 0 –13.0–14.9^{++}	77.9–0 –14.6–7.5		
	1523 K	$\gamma + \gamma'$	75.7– 0 –14.5– 9.8	75.8– 0 –13.5–10.7	74.8–0 –20.1–5.1		
	1273 K	$\gamma + \gamma' + \delta'$	76.0– 0 –14.2– 9.8	77.2– 0 –12.9– 9.9	75.4–0 –19.4–5.2	50.3–0–0.01–49.6	
	1073 K‡	$\gamma + \gamma' + \delta''$	76.3– 0 –13.6–10.1	77.7– 0 –13.8– 8.5	75.2–0 –18.9–5.9		74.6–0–7.0–18.4
			(76.0– 0 –14.1– 9.9)				
2	As-cast	γ, (γ')	75.7–10.3–14.0– 0	75.7–10.3–14.0– 0$^{++\Delta}$	⊕		
	1523 K	γ, (γ')	75.5–10.1–14.4– 0	75.5–10.1–14.4– 0	⊕		
	1273 K	$\gamma + \gamma'$	76.0– 9.8–14.2– 0	76.5–11.8–11.7– 0$^{\Delta}$	74.5–7.2–18.3–0$^{\Delta}$		
	1073 K	$\gamma + \gamma'$	76.3– 9.8–13.9– 0	76.7–11.8–11.5– 0$^{\Delta}$	76.1–8.9–15.0–0$^{\Delta}$		
			(75.9– 9.9–14.2– 0)				
3	As-cast	$\gamma + (\gamma') + \dagger$	76.4– 2.6–18.4– 2.6	77.3– 2.7–17.7– 2.3^{++}	⊕		
	1523 K	$\gamma + \gamma'$	75.5– 2.4–19.8– 2.3	76.6– 3.6–16.6– 3.2	74.8–2.2–20.8–2.2		
	1273 K	γ'	75.2– 2.3–19.9– 2.6		75.2–2.3–19.9–2.6		
	1073 K	γ'	75.9– 2.6–18.9– 2.6		75.9–2.6–18.9–2.6		
			(75.5– 2.5–19.5– 2.5)				
4	As-cast	γ, (γ')	77.4– 5.0–12.5– 5.1	78.2– 4.9–12.4– 4.5^{++}	⊕		
	1523 K	γ, (γ')	76.3– 4.7–14.2– 4.8	76.3– 4.7–14.2– 4.8	⊕		
	1273 K	$\gamma + \gamma'$	75.8– 4.7–14.5– 5.0	76.1– 6.5–11.4– 6.0	74.7–3.6–17.2–4.5		
	1073 K	$\gamma + \gamma'$	76.2– 4.1–14.8– 4.9	77.3– 6.3–10.6– 5.8	76.0–3.5–16.3–4.2		
			(76.1– 4.5–14.5– 4.9)				
5	As-cast	γ, (γ')	76.5– 7.7– 8.3– 7.5	76.5– 7.7– 8.3– 7.5^{++}	⊕		
	1523 K	γ	76.0– 7.2– 9.5– 7.3	76.0– 7.2– 9.5– 7.3			
	1273 K	$\gamma + \gamma'$	75.5– 7.3– 9.4– 7.8	76.2– 7.6– 8.2– 8.0	74.2–3.5–17.9–4.4		
	1073 K	$\gamma + \gamma'$	75.9– 7.4– 8.9– 7.8	76.4– 8.5– 6.8– 8.3	75.3–5.6–12.9–6.2		
			(75.8– 7.3– 9.3– 7.6)				

*Mo-rich regions present: composition 57.8Ni–9.5Al–32.7Mo (at %).

†Ni-rich β (based on NiAl) phase present. Composition: 65.2Ni–2.3Cr–32.1Al–0.4Mo (at %). $^{++}$Indicates primary phase in the as-cast structure (compositions represent dendrite centres).

‡The data refer to annealing at 1073 K without prior annealing at 1273 K. The composition of γ phase was measured in regions as close as possible to the Ni_3Mo phase; in other regions where γ adjoined γ', the aluminium content was lower (i.e. ~ 10.9 at %) and the molybdenum content higher (i.e. ~ 10.7 at %).

( ) Alloy composition data in brackets represent average of heat treated samples. $^{\Delta}$Result prone to error due to small particle size and/or presence of fine second phase particles. (γ'), ⊕ Precipitated during quenching/cooling.

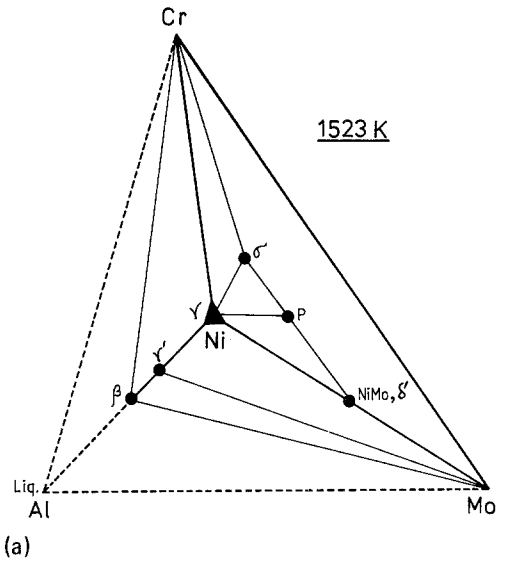

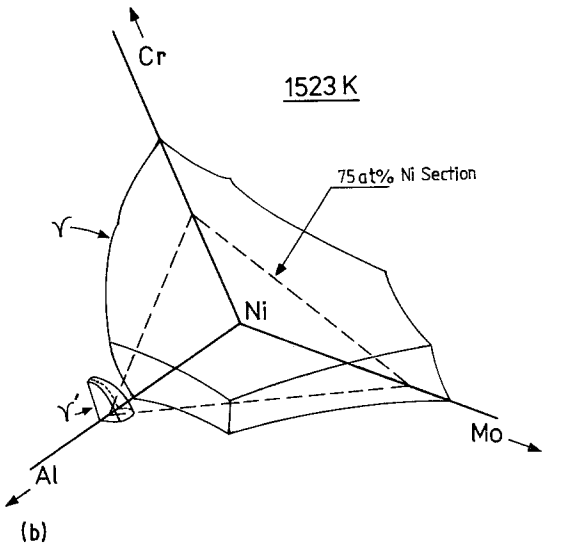

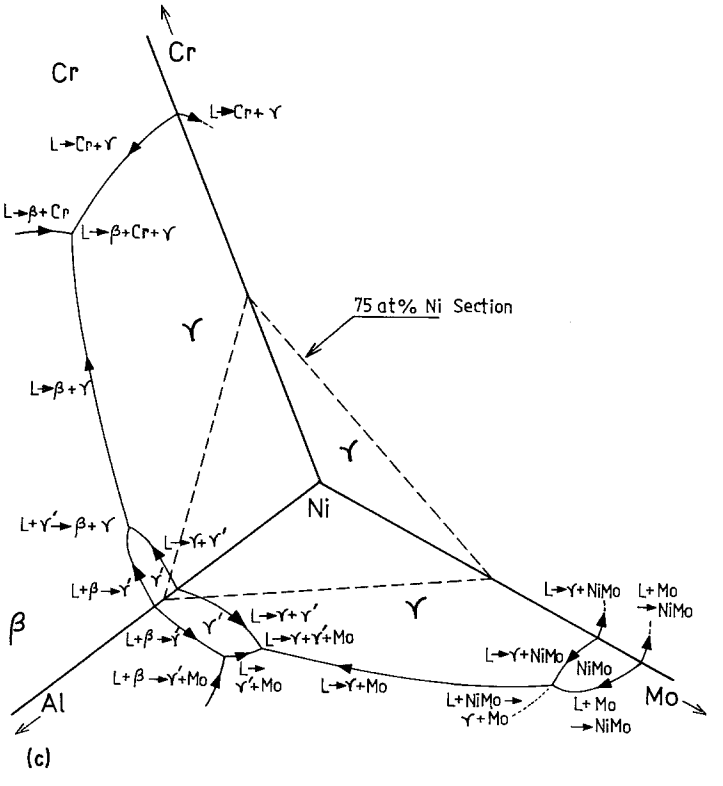

Figure 1 Nickel-rich portion of the Ni–Cr–Al–Mo system at 1523 K viewed towards the nickel-rich corner of the isothermal tetrahedron. (a) Schematic representation of the phases present in three of the constituent systems i.e. Ni–Al–Cr, Ni–Al–Mo, Ni–Cr–Mo, showing 3-phase tie triangles based on experimental data [2, 12, 24, 26, 31]. The full extent of the single phase regions is not shown and the 2-phase regions are represented by straight lines. The 3-phase tie triangles for γ, δ', Mo and γ, γ', β are not shown, since with this method of representation, it is virtually coincident with the Ni–Mo edge of the tetrahedron. The Cr–Mo system shows complete solid solubility. Possible forms of the equilibrium regions in the quaternary system are not shown. (b) Schematic representation showing the approximate forms of the single phase regions in the Ni–Al–Cr, Ni–Al–Mo, Ni–Cr–Mo systems. ----- represents 75 at% Ni section. (c) Schematic representation of the liquidus projections for the Ni–Al–Mo, and Ni–Al–Cr systems. These projections are based on previously reported experimental work for the Ni–Al–Cr and Ni–Al–Mo systems [2, 24]. Experimental data are available for the Ni–Cr–Mo system [26]; the proposed liquidus equilibria are complex and are not shown here.

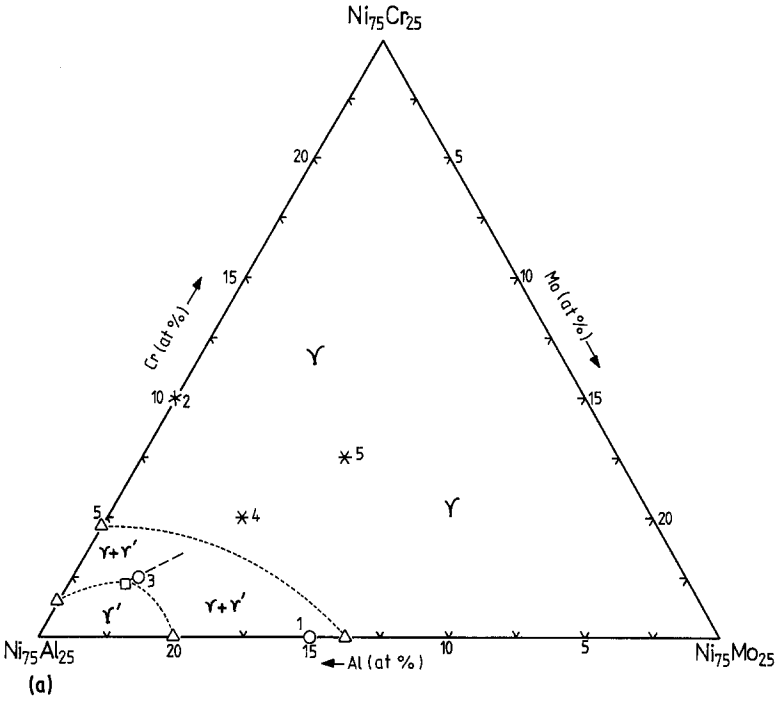

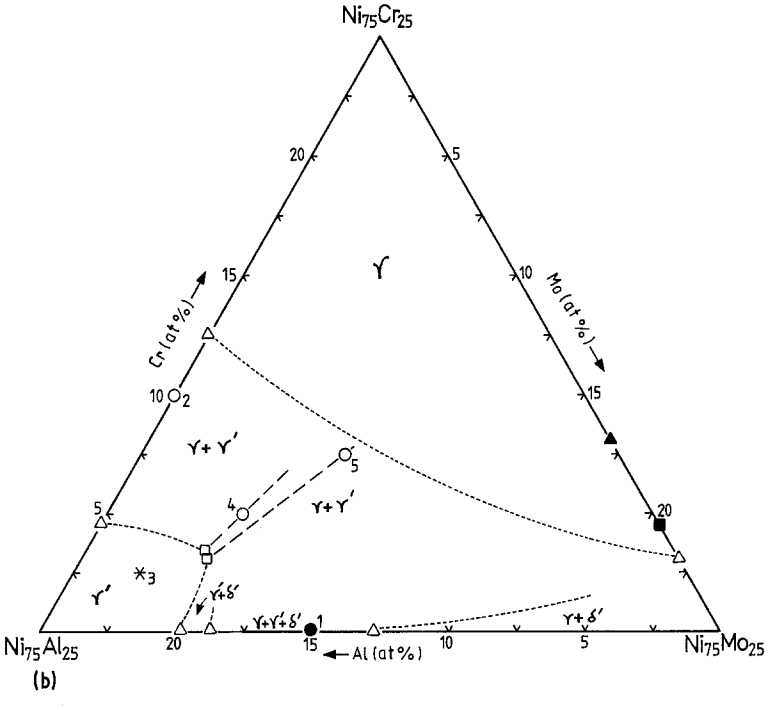

Figure 2 Partial isothermal section of the Ni–Cr–Al–Mo system at a nickel content of 75 at%: (a) 1523 K, (b) 1273 K, and (c) 1073 K. △ Data for the Ni–Al–Cr ternary system are from [2]. △ Data for the Ni–Al–Mo ternary system are from the present work and from [25]. Data from [17] show some differences in boundary positions from those shown here. At 1073 K, a small $\gamma + \delta''$ region [38] is not included here. Experimental data for the Mo-rich corner at 1073 K are lacking and the boundaries shown are estimated to indicate the type of equilibrium expected. △ Data for the Ni–Cr–Mo ternary system are derived for (a) [31] and for (b), (c) from binary Ni–Mo and Ni–Cr data [36, 37]. In addition γ boundary points by [34] at 1173 K and by [35] at 1073 K are shown by ▲ and ▼ symbols, respectively. Data point at 1123 K [31] is also presented by symbol ■. The only phase composition data points included in Fig. 2 are those lying close to the 75 at% Ni section i.e. within ~ ± 0.5 at%. Concerning alloy 4 at 1073 K the structure was found to be $\gamma + \gamma'$ (Fig. 7); but the nickel contents of $\gamma + \gamma'$ were significantly higher than 75 at%. The data for this alloy have not, therefore, been used to define the boundary of the γ' region. Instead the boundary has been drawn on the basis of data for alloy 5 where the γ' composition is close to the 75 at% Ni section. □ Phase composition by EPMA; ----- interpolated phase boundary; – – – – tie lines determined by EPMA; △ data from previous work; * single phase alloy; ○ composition of 2 phase alloy; • composition of 3 phase alloy.

progressively along the chromium axis from the $Ni_{75}Al_{25}$ corner in the direction of decreasing aluminium content. At these lower temperatures, the γ field correspondingly diminishes, along the chromium axis. Also from the molybdenum axis and the $Ni_{75}Cr_{25}$–$Ni_{75}Mo_{25}$ axis intermetallic compounds (NiMo, $Ni_3Mo(\delta'')$, σ and P phase) intervene in the γ field. The present results provide no information on intermetallic compounds in the quaternary alloys.

In the two phase γ and γ' region, the tie lines for the quaternary alloys generally deviated by up

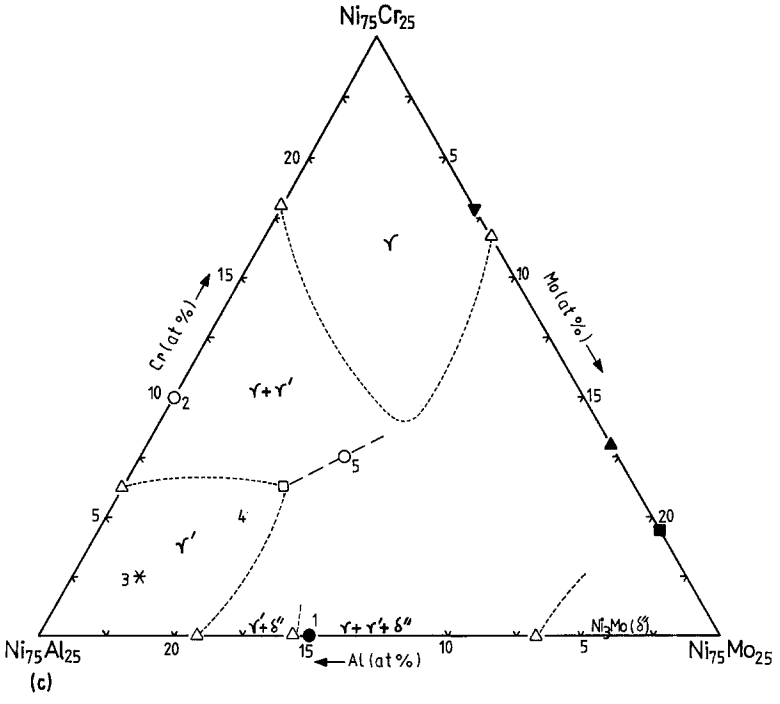

Figure 2 Continued.

to ~ 1 at% from the average alloy compositions and it is thus difficult to represent accurately the boundaries of the phase regions. The γ in the quaternary alloys tends to lie at nickel rich levels and the γ' at nickel poor levels relative to the average alloy compositions.

Concerning the location of the boundaries of the $\gamma + \gamma'$ region in the ternary Ni–Al–Cr system, the points shown have been taken from the work of Taylor and Floyd [2]. The compositional data for the Ni–Al–Cr alloy in the present work at 1073 K agree well with Taylor and Floyd even though the accuracy is limited by the small γ' particle size; however, the γ composition measured in the $\gamma + \gamma'$ structure produced by 1273 K annealing does not agree closely with Taylor and Floyd [2], but is in reasonable agreement with DeLanerolle and Seigle [13] at 1298 K. The single phase γ at 1523 K is consistent with Taylor and Floyd's data for 1423 K [2].

In the case of the Ni–Al–Mo alloy the results reported here for γ' at 1523 K agree reasonably with the work of Nash *et al.* [24]; however, the γ composition determined at 1523 K lies at a lower aluminium content than is indicated by this previous data [24]. For 1273 K the presence of NiMo indicating equilibrium between γ, γ' and NiMo is in agreement with recent work [25] and thus suggests the occurrence of the $\gamma + \text{Mo} \rightarrow \gamma' + \text{NiMo}$ reaction (Fig. 3). On annealing at 1073 K without prior annealing at 1273 K, the structure consists of $\gamma + \gamma' + \delta''$ (Ni_3Mo) (Tables I and II). Ni_3Mo shows a lamellar type of precipitation within the γ phase. Details of this structure are to be reported elsewhere [38]. This observation contrasts with the work of Markiv *et al.* [18] who reported equilibrium between γ, γ' and molybdenum in the composition range in which alloy 1 lies.

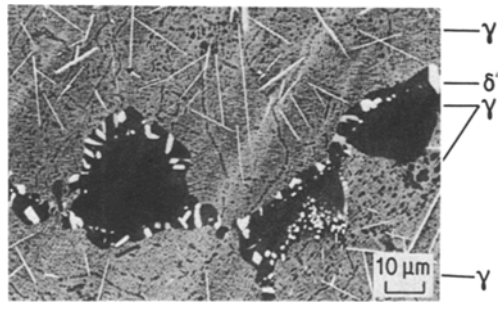

Figure 3 Alloy 1, Ni–15Al–10Mo, annealed at 1273 K for 1 week after 1523 K, 1 week treatment. Large γ' phase particles (dark) are retained from 1523 K treatment in a γ matrix (grey). In addition, solid state precipitation of fine γ' particles (dark) along with acicular and "blocky" forms of NiMo precipitation (white) are evident at this temperature; the "blocky" particles form near the edges of the large γ' regions. High resolution back-scattered electron image, unetched.

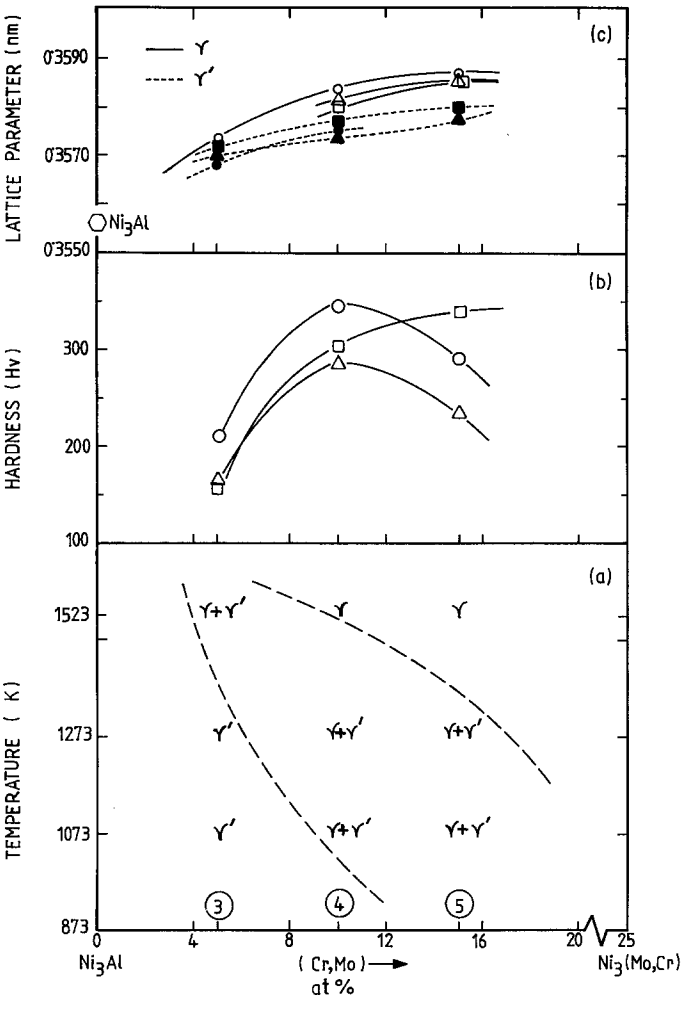

Figure 4 Data for alloy series 3, 4, 5 along the line $Ni_{75}Al_{25}$ to Ni_{75} ($Cr_{12.5}Mo_{12.5}$) representing decreasing aluminium content at a constant Cr:Mo ratio. (a) Approximate form of vertical section of the 75 at% Ni section of the quaternary system. (b) Hardness data. (c) $\gamma + \gamma'$ lattice parameter data. Heat treatment temperatures are ○ 1523 K, △ 1273 K, and □ 1073 K. Open symbols γ; closed symbols γ'.

Loomis *et al.* [10] have studied γ, γ' relationships in certain Ni–Cr–Al–Mo alloys: the $\gamma/\gamma + \gamma'$ boundaries reported for alloys with nickel contents between ~ 75 and 76 at% Ni agree reasonably well with the present work.

4.2. Vertical sections

Figs. 4a and 5a show the data in the form of vertical sections, although phase boundary regions are not accurately bracketed.

The section containing alloys 3, 4 and 5 (Fig. 4a) illustrates the expansion of the γ' field with decreasing temperature. Thus, alloy 3 consisted of $\gamma + \gamma'$ at 1523 K but was single phase γ' at the lower temperatures. The γ' composition in alloy 3 with respect to molybdenum and chromium was virtually independent of temperature, while the aluminium content showed a decrease accompanied by an increase in nickel. Alloy 4 was interpreted as single phase γ at 1523 K and was two phase $\gamma + \gamma'$ at the lower temperatures. In alloy 4, the γ showed a trend towards an increase in molybdenum and chromium and a decrease in aluminium with decreasing temperature; for γ' there was no significant variation in molybdenum and chromium while the nickel and aluminium variations showed no clear trend. Alloy 5 consisted of γ at 1523 K but became $\gamma + \gamma'$ with increasing amounts of γ' with decreasing temperature. The γ composition tended to increase in molybdenum and chromium and to decrease in aluminium as the temperature decreased; the γ' also showed an increase in molybdenum and chromium with an unexpected marked decrease in aluminium.

In the section consisting of alloys 2, 4 and 1, each alloy contained 15 at% Al (Fig. 5a). In the Ni–Cr–Al alloy (2), the alloy was single phase γ at 1523 K (although γ' formed during quenching), and $\gamma + \gamma'$ at the lower temperatures; the γ composition showed a decrease in aluminium content

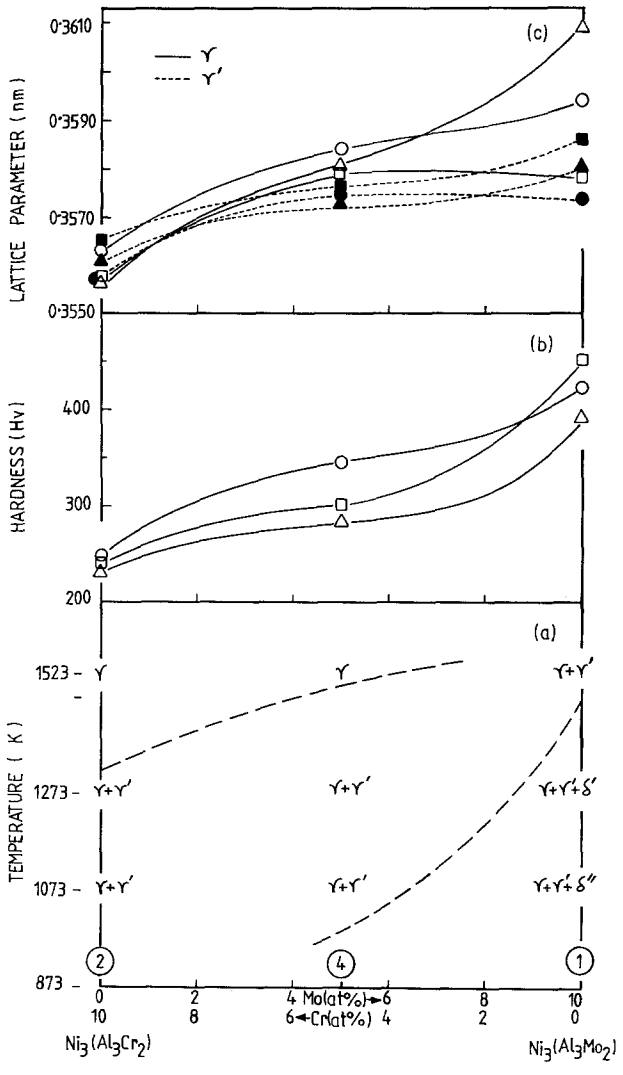

Figure 5 Data for alloy series 2, 4, 1 representing constant aluminium content (15 at %). (a) Approximate form of vertical section of the 75 at % Ni section of the quaternary system. The boundaries separating the regions containing δ'(NiMo) and δ''(Ni_3Mo) have not been determined. (b) Hardness data. (c) $\gamma + \gamma'$ lattice parameter data heat treatment temperatures are ○ 1523 K, △ 1273 K, and □ 1073 K. Open symbols γ; closed symbols γ'.

and an increase in chromium content as the temperature decreased from 1523 to 1273 K. The Ni–Al–Mo alloy (1) consisted of $\gamma + \gamma'$ at 1523 K, while at 1273 K, NiMo was also present; the γ' and γ showed a small decrease in aluminium and molybdenum content, respectively, with decreasing temperature. Ni_3Mo was present at 1073 K in place of NiMo; but the boundaries separating the regions containing NiMo and Ni_3Mo, respectively, have not been determined.

4.3. Lattice parameter and hardness data

Table I and Figs. 4c, 5c show the lattice parameter for the γ and γ' phases. In view of the γ and γ' lattice parameter being so close, it should be noted that successful identification and lattice parameter determination of γ, and γ' were only possible on the basis of (100), (110), (210) and (211) reflections which are characteristic of γ' superlattices only.

The alloy series 2, 4, 1, representing increasing molybdenum content of the alloy at a constant aluminium content of 15 at % shows a small increase in the γ lattice parameter (Fig. 5c). This is consistent with the large atomic diameter of molybdenum (0.147 nm) and the increase in molybdenum content of the γ phase from 0 to 10 at % Mo (Table II). There is an exception for the 1073 K treatment, where γ in alloy 1 has a slightly smaller parameter than in alloy 4. In the γ' also the parameter increases with the molybdenum content of the phase.

In the alloy series 3, 4, 5 representing a decrease in aluminium content at constant Cr/Mo ratio,

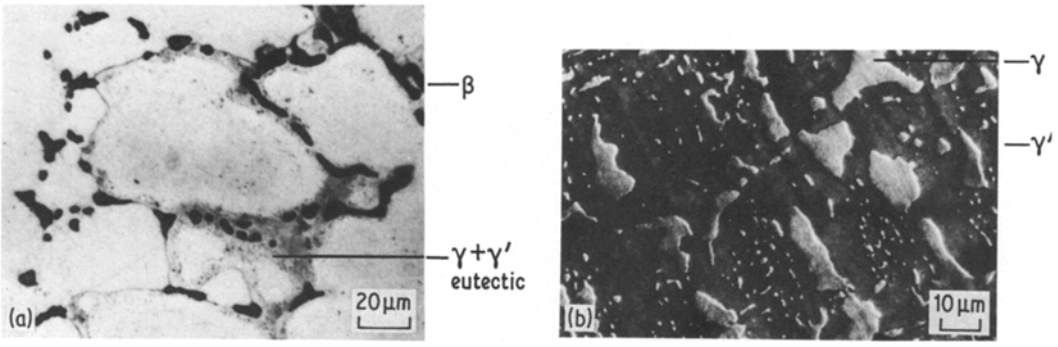

Figure 6 Alloy 3, Ni–2.5Cr–20Al–2.5Mo: (a) as-cast structure which is predominantly γ dendrites with interdendritic β present (dark etching) together with regions which may be γ/γ' eutectic (etched $FeCl_3$/ethanol), optical micrograph; (b) annealed 1523 K 1 week, showing bi-modal dispersion of γ in a matrix of γ' (dark appearance) (etched $FeCl_3$/ethanol). SEM.

there is a small progressive increase in γ and γ' parameters (Fig. 4c) which also follows a reasonably consistent correlation with increase in molybdenum content of the individual phases [10].

The γ/γ' mismatch values in the heat treated ternary Ni–Al–Mo alloy are negative after annealing at 1523 and 1273 K (i.e. the γ' parameter is less than that of γ); the values are -0.56 and -0.83%, respectively. These relatively large values are attributed mainly to the difference of ~ 5 at % in the molybdenum contents of the two phases (Table II); the higher content of molybdenum in the γ phase significantly expands the lattice parameter. After annealing at 1073 K the γ/γ' mismatch in the ternary Ni–Al–Mo alloy (1) shows a small positive value (0.20%) associated with a significant decrease in γ lattice parameter. The effect is thought to be due mainly to a depletion of the γ phase in molybdenum resulting from the $Ni_3Mo(\delta'')$ precipitation, but the plate like formation of Ni_3Mo is on too fine a scale for accurate electron probe microanalysis of the associated γ to be carried out. The mismatch values in the quaternary alloys (3, 4, 5) are small and negative, lying between -0.14 and -0.25. This feature also can be correlated approximately with the smaller Mo content difference between the γ and γ' in 3 and 4; however, the correlation is not good in the case of alloy 5, where there is a larger difference in molybdenum content. In the ternary Ni–Al–Cr alloy, there is a small positive mismatch (~ 0.1 to 0.2%). The data agree well with the work of Taylor and Floyd [2] who reported the coexistence of γ and γ' of equal parameters over a range of compositions in this system. The γ' parameter of 0.3565 nm in the present work for the Ni–Al–Cr alloy annealed at 1073 K agrees well with the value of 0.3559 nm reported by Taylor and Floyd [2] for an alloy of the same composition annealed at the same temperature; it also agrees well with the results of Arbuzov and Zelenkov [21].

The interpretation of the hardness data (Figs. 4b and 5b) is hindered by lack of data on fine scale solid state precipitation. The Ni–Al–Mo alloy shows the highest hardness of the alloys studied: the increase in hardness after annealing at 1073 K is attributed to Ni_3Mo precipitation. In alloy series 3–5, alloy 3 consisting mainly or entirely of γ' has a relatively low hardness. The data for alloy 2 agree well with that reported by Arbuzov and Zelenkov [21] for an alloy of the same composition quenched from 1273 K; these workers, however, reported the structure as γ' not $\gamma + \gamma'$. Alloy 4 consisting of $\gamma + \gamma'$ with γ' dispersions shows a higher value, while there is a decrease in hardness in alloy 5 which has the greatest γ content in the series.

4.4. Microstructural features

All of the alloys appeared to solidify predominantly as cored single phase structures. Only in the ternary Ni–Al–Mo alloy 1 and in quaternary alloy 3 was there clear evidence that a second phase formed during solidification, as distinct from during subsequent solid state cooling. Thus, alloy 1 in the as-solidified state contain molybdenum rich regions [16] while in alloy 3, β(NiAl) phase was detected and possibly γ/γ' eutectic (Fig. 6 and Table II). However, X-ray diffraction showed the presence of both γ and γ' in the as-solidified state in all of the alloys. In the two ternary alloys consideration of the phase diagram

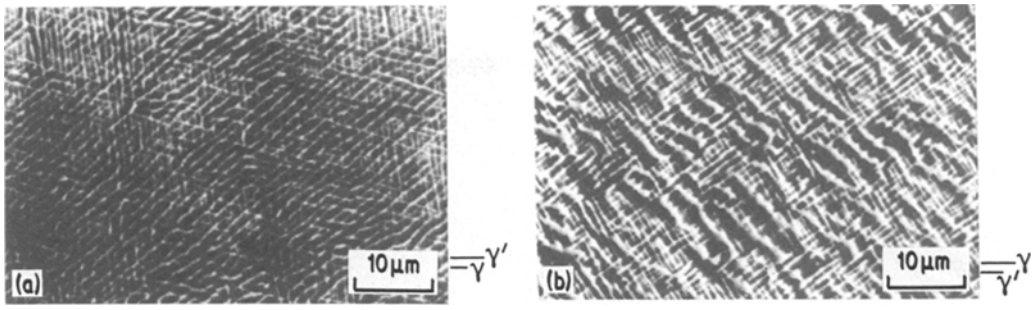

Figure 7 Alloy 4, Ni–5Cr–15Al–5Mo, (a) annealed at 1273 K for 1 week, and (b) annealed at 1073 K for 1 week after 1273 K treatment. Raft-like γ' structure (dark) in γ matrix. Raft length ~ 10 to 12 μm. Raft width ~ 1 to 1.5 μm in (a) 1 to 3 μm in (b). Etched in $FeCl_3$/ethanol. SEM.

data in the literature indicates the primary phase to be γ; the presence of γ' is interpreted as resulting mainly or entirely from solid state precipitation. It is probable that the primary phase is also γ in each of the quaternary alloys and that where a few particles were observed these were γ' formed in the solid state; for example, the as-cast sample of alloy 3 when viewed by optical microscopy showed a fine particle dispersion of the order of 1 μm size. In the absence of transmission electron microscopy results, detailed interpretation of the as-cast structures cannot be made.

Structures produced by annealing are illustrated in Figs. 6b, 7 and 8. In alloy 3, annealed at 1523 K, the predominant phase was γ', and there was a bimodal dispersion of irregular shaped particles of γ (Fig. 6b); annealing had removed the β phase. Alloys 4 and 5 annealed at 1273 and 1073 K consisted of $\gamma + \gamma'$ structures (Figs. 7 and 8). Alloy 4 contained a greater volume fraction of γ'. The γ' dispersions were raft-like in nature [10], each raft apparently having formed by directional coarsening of a number of γ' cuboids. The average raft length in alloy 4 was in the range ~ 10 to 12 μm as compared with ~ 2 to 5 μm in alloy 5. Raft widths (corresponding to the dimension of an individual γ' cuboid) were in the range ~ 0.7 to 3 μm and there was little difference in raft width between alloys 4 and 5. There was a trend for raft width (and, less clearly, raft length) to be increased by annealing at 1073 K for 1 week after annealing at 1273 K for 1 week; this is attributed mainly to an increase in the volume fraction of γ' produced by the 1073 K annealing, rather than to a normal coarsening process.

γ' "raft" formation has been studied in nickel-based superalloys, resulting from directional coarsening under stress at elevated temperatures, e.g. [39–42]; Ni–Al–Mo–Ta alloys showing large negative γ/γ' mismatch values are among materials investigated. The present results show that γ' rafts can form on prolonged annealing at 1273 K without the application of stress. The raft dimensions are considerably larger than those reported in

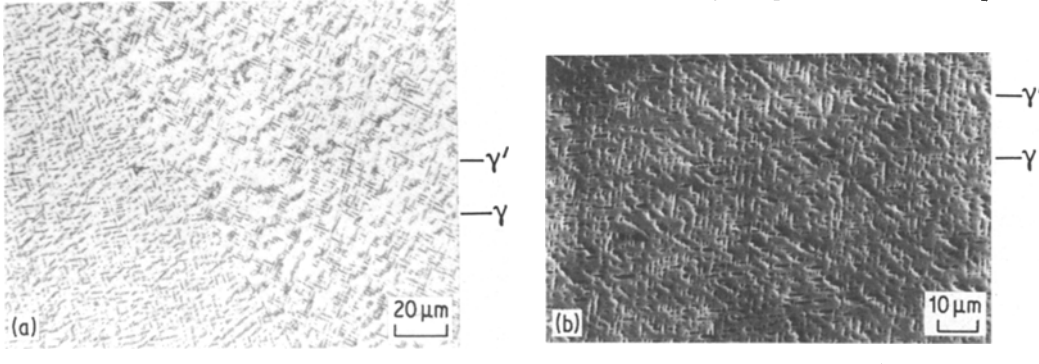

Figure 8 Alloy 5, Ni–7.5Cr–10Al–7.5Mo, (a) annealed at 1273 K for 1 week, and (b) annealed 1073 K, 1 week after 1273 K treatment. Raft like γ' structure (dark) in γ matrix. Lower volume fraction of γ' than in alloy 4. Raft length (a) 2 to 3 μm. (b) 3 to 5 μm. Raft width (a) 0.7 to 2 μm. (b) 1 to 2.5 μm. Etched $FeCl_3$/ethanol (a) optical micrograph, (b) SEM.

previous studies where the annealing temperatures were lower. It should be noted that rafts form in the quaternary Ni–Cr–Al–Mo alloys (4 and 5) which show small negative mismatch values, whereas in the ternary Ni–Al–Cr alloy (2) which has a small positive mismatch, raft formation has not clearly developed.

The coarsening rate of γ' has not been studied in the present work. However, it is of interest to compare the present observations with studies of γ' coarsening in IN 738 alloy [43–45]. The γ' cuboid size of alloys 4 and 5 annealed for 1 week at 1273 K lay in the range ~ 0.7 to 2 μm, which is larger than that reported by Rosenthal [45] for IN 738 annealed for 15 days at 1323 K (i.e. 0.75 μm). The low mismatch in alloys 4 and 5 should favour resistance to coarsening; however, the influence of diffusion in achieving the necessary partitioning of alloy elements may be less effective in retarding coarsening in the quaternary alloys than in the more complex alloy containing a range of slow diffusing elements.

5. Conclusions

The constitution of the Ni–Cr–Al–Mo system in the 75 at% Ni section at 1523 K consists of phase fields containing γ', $\gamma' + \gamma$, and γ; the γ phase occupies the major part of the system, i.e. for alloy compositions with greater than ~ 5 at% Cr and ~ 17 at% Mo. The maximum extent of the γ' region lies at ~ 2.5 at% Cr, 2.5 at% Mo. With decreasing temperature (1273 and 1073 K), the γ' and $\gamma' + \gamma$ fields expand at the expense of the γ field. The maximum extent of the γ' region lies at ~ 5 at% Cr, 5 at% Mo at 1073 K. At the lower temperatures other phases appear in the quaternary system, although these were not studied in the present work. The quaternary γ/γ' alloys showed small lattice mismatch values (up to $\sim 0.25\%$); the γ' parameter being less than that of γ, i.e. negative mismatch. In the ternary Ni–Al–Mo alloy studied δ'(NiMo) precipitated at 1273 K and δ''(Ni_3Mo) at 1073 K.

Acknowledgements

The authors would like to thank Professor D. W. Pashley for the provision of research facilities and SERC for support of the work.

References

1. E. S. MACHLIN and J. SHAO, *Met. Trans.* 9A (1978) 561.
2. A. TAYLOR and R. W. FLOYD, *J. Inst. Met.* 81 (1952–53) 451.
3. A. TAYLOR, *Trans. AIME J. Met.* 206 (1956) 1356.
4. I. I. KORNILOV and R. S. MINTS, *Akad. Nauk. SSSR Izvest. Sektora Fiz-khim. Anal. Obshchei Neorg. Khim.* 26 (1955) 62.
5. Yu. A. BAGARYATSKIY, Z. M. PETROVA and L. M. UTEVSKIY, *Prob. Met. Fiz. Metal. Inst. Metalloved. Fiz. Metall. Sbornik Trudov* 5 (1958) 235.
6. Yu. A. BAGARYATSKIY, *Zhur. Neorg. Khim.* 3 (1958) 722.
7. I. I. KORNILOV and R. S. MINTS, *ibid.* 3 (1958) 699.
8. C. M. HAMMOND, R. A. FLINN and L. THOMASSEN, *Trans. Met. Soc. AIME* 221 (1961) 400.
9. L. KAUFMAN and H. NESOR, *Met. Trans.* 5 (1974) 1623.
10. W. T. LOOMIS, J. W. FREEMAN and D. L. SPONSELLER, *ibid.* 3 (1972) 989.
11. R. KADALBAL, J. MONTOYA-CRUZ and T. Z. KATTAMIS, "Rapid Solidification Processing, Principles and Technologies II", edited by R. Mehrabian, B. H. Kear and M. Cohen (Claitors Publishing Division, Baton Rouge, 1980) p. 195.
12. S. M. MERCHANT and M. R. NOTIS, *Bull. Alloy Phase Diagrams*, to be published.
13. N. DELANEROLLE and L. L. SEIGLE, unpublished work (1983).
14. D. C. TU, PhD thesis, SUNY at Stony Brook (1982).
15. B. B. ARGENT, C. W. HAYWORTH and N. C. OFORKA, private communication (1984).
16. S. CHAKRAVORTY and D. R. F. WEST, *Met. Sci.* 18 (1984) 207.
17. D. B. MIRACLE, K. A. LARK, V. SRINIVASAN and H. A. LIPSITT, *Met. Trans.* 15A (1984) 481.
18. V. Ya MARKIV, V. V. BURNASHOVA, L. I. PRYAKHINA and K. P. M. MYASNIKOVA, *Izvest. Akad. Nauk SSSR Met.* 5 (1969) 180.
19. A. V. VIRKAR and A. RAMAN, *Z. Metallk.* 60 (1969) 594.
20. Yu. A. BAGANYATSKIY and L. E. IVANOVSKAYA, *Doklady Akad. Nauk SSSR* 132 (1960) 339.
21. M. P. ARBUZOV and I. A. ZELENKOV, *Fiz. Met. Metalloved.* 15 (1963) 725.
22. H. E. CLINE and J. L. WALTER, *Met. Trans.* 1 (1970) 2907.
23. E. H. AIGELTINGER, S. R. BATES, R. W. GOULD, J. J. HREN and F. N. RHINES, "Rapid Solidification Processing, Principles and Technologies", edited by R. Mehrabian, B. H. Kear and M. Cohen (Claitor's Publishing Division, Baton Rouge, 1978) p. 291.
24. P. NASH, S. FIELDING and D. R. F. WEST, *Met. Sci.* 17 (1983) 192.
25. K. WAKASHIMA, K. HIGUCHI, T. SUZUKI and S. UMEKAWA, *Acta. Metall.* 31 (1983) 1937.
26. D. S. BLOOM and N. J. GRANT, *Trans. AIME J. Met.* (1954) 261.
27. S. R. RIDEOUT and P. A. BECK, US Advisory Committee for Aeronautics Technical Note 2683 (1952).

28. S. R. RIDEOUT, W. D. MANLY, E. L. KAMEN, B. S. LEMENT and P. A. BECK, *Trans. AIME J. Met.* **191** (1951) 872.
29. C. BRINK and D. P. SHOEMAKER, *Acta. Crystallogr.* 8 (1955) 734.
30. D. P. SHOEMAKER, C. B. SHOEMAKER and F. C. WILSON, *ibid.* **10** (1957) 1.
31. M. RAGHAVAN, R. R. MUELLER, G. A. VAUGHN and S. FLOREEN, *Met. Trans.* **15A** (1984) 783.
32. L. KAUFMAN and H. NESOR, *ibid.* **5** (1974) 1617.
33. R. G. BARROWS and J. B. NEWKIRK, *ibid.* **3** (1972) 2889.
34. J. R. MIHALISIN, C. G. BIEBER and R. T. GRANT, *Trans. AIME* **242** (1968) 2399.
35. A. P. SMIRYAGIN, A. YA. POTEMKIN and R. P. MARTINUK, *Zhur. Neorg. Khim.* **3** (1958) 853.
36. F. A. SHUNK, "Constitution of Binary Alloys", 2nd Supplement (McGraw Hill, New York, 1969) p. 273, 515.
37. M. HANSEN and K. ANDERKO, "Constitution of Binary Alloys" 2nd edn (McGraw Hill, New York, 1958) p. 541.
38. S. CHAKRAVORTY and D. R. F. WEST, to be published.
39. J. K. TIEN and S. M. COPLEY, *Met. Trans.* **2** (1971) 543.
40. J. K. TIEN and R. P. GAMBLE, *ibid.* **3** (1972) 2157.
41. D. D. PEARSON, F. D. LEMKEY and B. H. KEAR, Proceedings 4th International Symposium on Superalloys, edited by J. K. Tien, S. T. Wlodek, H. Morrow, M. Gell and G. E. Maurer (ASM, Metals Park, 1980) p. 513.
42. R. A. MacKAY and L. J. EBERT, *Scripta Metall.* **17** (1983) 1217.
43. R. A. STEVENS and P. E. J. FLEWITT, *J. Mater. Sci.* **13** (1978) 367.
44. R. A. STEVENS and P. E. J. FLEWITT, *Mat. Sci. Eng.* **37** (1979) 237.
45. R. ROSENTHAL, PhD thesis, University of London (1983).

Received 28 December 1983
and accepted 16 January 1984